

Załącznik nr 3

Study of the properties of neutron-rich isotopes  
in the neighbourhood of the doubly magic nuclei  
 $^{78}\text{Ni}$  and  $^{132}\text{Sn}$

Scientific Curriculum Vitae (Autoreferat)

Agnieszka Korgul

Nuclear Physics Division  
Institute of Experimental Physics  
Faculty of Physics  
University of Warsaw



## CONTENTS

<b>1</b>	<b>Name and Surname</b>	<b>2</b>
<b>2</b>	<b>Qualifications</b>	<b>2</b>
<b>3</b>	<b>Information on employment at scientific institutions</b>	<b>2</b>
<b>4</b>	<b>Research and results related to the habilitation topic. Achievements resulting from art. 16 par. 2 of the act of March 14th, 2003 on academic degrees and scientific title on scientific degrees and titles in the field of art (Dz. U. No. 65, item 595 as amended)</b>	<b>2</b>
4.1	Habilitation-topic title . . . . .	2
4.2	Publications selected for the habilitation process . . . . .	3
4.3	Scientific motivation and results from the selected publications and future plans.	5
4.3.1	Scientific motivation . . . . .	5
4.3.2	Experimental techniques . . . . .	9
4.3.3	Results . . . . .	10
4.3.4	Summary and outlook on future research . . . . .	19
<b>5</b>	<b>Other scientific interests</b>	<b>21</b>
5.1	Scientific interests during the studies . . . . .	21
5.1.1	Master studies . . . . .	21
5.1.2	Doctoral studies . . . . .	22
5.2	Other scientific interests after the end of doctoral studies . . . . .	23
5.2.1	Properties of neutron-deficient nuclei close to $^{100}\text{Sn}$ . . . . .	23
5.2.2	Rare decay modes of exotic nuclei . . . . .	24
5.2.3	Structure of nuclei close to the semi-magic $^{68}\text{Ni}$ . . . . .	25
5.2.4	Properties of nuclei studied with the fast timing technique . . . . .	25

## 1 NAME AND SURNAME

Agnieszka Barbara Korgul

## 2 QUALIFICATIONS

### a) Master diploma, 1997

Faculty of Physics, University of Warsaw

Thesis title: *Study of the production of microsecond isomeric states in the fragmentation reaction of  $^{86}\text{Kr}$  (Badanie produkcji mikrosekundowych stanów izomerycznych w reakcji fragmentacji  $^{86}\text{Kr}$ )*,

supervisor: prof. Andrzej Płochocki

### b) Doctoral degree in Physics Sciences, 2002

Faculty of Physics, University of Warsaw

Thesis title: *Single-particle energies in the neighbourhood of the doubly magic nucleus  $^{132}\text{Sn}$  (Energie jednocząstkowe w okolicy podwójnie magicznego jądra  $^{132}\text{Sn}$ )*,

supervisor: prof. Waldemar Urban

## 3 INFORMATION ON EMPLOYMENT AT SCIENTIFIC INSTITUTIONS

### a) Faculty of Physics, University of Warsaw, since 2003

### b) University of Tennessee, 01.03.2005 - 28.02.2006

## 4 RESEARCH AND RESULTS RELATED TO THE HABILITATION TOPIC. ACHIEVEMENTS RESULTING FROM ART. 16 PAR. 2 OF THE ACT OF MARCH 14TH, 2003 ON ACADEMIC DEGREES AND SCIENTIFIC TITLE ON SCIENTIFIC DEGREES AND TITLES IN THE FIELD OF ART (Dz. U. NO. 65, ITEM 595 AS AMENDED)

### 4.1 HABILITATION-TOPIC TITLE

**Study of the properties of neutron-rich isotopes in the neighbourhood of the doubly magic nuclei  $^{78}\text{Ni}$  and  $^{132}\text{Sn}$ .**

#### 4.2 PUBLICATIONS SELECTED FOR THE HABILITATION PROCESS

- H1. **A. Korgul**, K. P. Rykaczewski, J. A. Winger, S. V. Ilyushkin, C. J. Gross, J. C. Batchelder, C. R. Bingham, I. N. Borzov, C. Goodin, R. Grzywacz, J. H. Hamilton, W. Królas, S. N. Liddick, C. Mazzocchi, C. Nelson, F. Nowacki, S. Padgett, A. Piechaczek, M. M. Rajabali, D. Shapira, K. Sieja, E. F. Zganjar,  
 *$\beta - \gamma$  and  $\beta$ -delayed neutron- $\gamma$  decay of neutron-rich copper isotopes*,  
Phys. Rev. C **86**, 024307 (2012).
- H2. **A. Korgul**, K. P. Rykaczewski, R. Grzywacz, H. Śliwińska, J. C. Batchelder, C. Bingham, I. N. Borzov, N. Brewer, L. Cartegni, A. Fijałkowska, C. J. Gross, J. H. Hamilton, C. Jost, M. Karny, W. Królas, S. Liu, C. Mazzocchi, M. Madurga, A. J. Mendez II, K. Miernik, D. Miller, S. Padgett, S. Paulauskas, D. Shapira, D. Stracener, K. Sieja, J. A. Winger, M. Wolińska-Cichocka, E. F. Zganjar,  
*Experimental study of the  $\beta$ - $\gamma$  and  $\beta$ - $n\gamma$  decay of the neutron-rich nucleus  $^{85}\text{Ga}$* ,  
Phys. Rev. C **88**, 044330 (2013).
- H3. **A. Korgul**, R. Grzywacz, K. P. Rykaczewski,  
*Structure of neutron-rich nuclei beyond  $N=50$* ,  
Acta Phys. Pol. B **45**, 223 (2014).
- H4. **A. Korgul**, K. P. Rykaczewski, R. Grzywacz, C. R. Bingham, N. Brewer, C. J. Gross, A. A. Ciemny, C. Jost, M. Karny, M. Madurga, C. Mazzocchi, A. J. Mendez II, K. Miernik, D. Miller, S. Padgett, S. Paulauskas, M. Piersa, D. Stracener, M. Stryjczyk, M. Wolińska-Cichocka, E. F. Zganjar,  
 *$\beta$  and  $\beta$ - $n$  decay of neutron-rich  $^{84}\text{Ge}$* ,  
Phys. Rev. C **93**, 064324 (2016).
- H5. **A. Korgul**, K. P. Rykaczewski, R. Grzywacz, C. R. Bingham, N. Brewer, C. J. Gross, C. Jost, M. Karny, M. Madurga, C. Mazzocchi, A. J. Mendez II, K. Miernik, D. Miller, S. Padgett, S. Paulauskas, M. Piersa, D. Stracener, M. Stryjczyk, M. Wolińska-Cichocka, E. F. Zganjar,  
*Study of the  $\beta$  and  $\beta$ - $n$  decay of the very neutron rich nucleus  $^{85}\text{Ge}$* ,  
Phys. Rev. C **95**, 044305 (2017).

- H6. **A. Korgul**, K. P. Rykaczewski, R. Grzywacz, C. R. Bingham, N. Brewer, C. J. Gross, A. A. Ciemny, C. Jost, M. Karny, M. Madurga, C. Mazzocchi, A. J. Mendez II, K. Miernik, D. Miller, S. Padgett, S. Paulauskas, D. Stracener, M. Wolińska-Cichocka, *Study of  $\beta$  and  $\beta$ -n decay of neutron-rich  $N=54$  isotone  $^{87}\text{As}$* , Phys. Rev. C **92**, 054318 (2015).
- H7. **A. Korgul**, H. Mach, B. A. Brown, A. Covello, A. Gargano, B. Fogelberg, W. Kurcewicz, E. Werner-Malento, R. Orlandi, M. Sawicka, *On the unusual properties of the 282 keV state in  $^{135}\text{Sb}$* , Eur. Phys. J. A **32**, 25 (2007).
- H8. **A. Korgul**, H. Mach, B. A. Brown, A. Covello, A. Gargano, B. Fogelberg, R. Schuber, W. Kurcewicz, E. Werner-Malento, R. Orlandi, M. Sawicka, *On the structure of the anomalously low-lying  $5/2^+$  state of  $^{135}\text{Sb}$* , Eur. Phys. J. A **25**, s01, 123 (2005).
- H9. **A. Korgul**, P. Bączyk, W. Urban, T. Rząca-Urban, A. G. Smith, I. Ahmad, *Investigation of the  $i_{13/2}$  neutron orbital in the  $^{132}\text{Sn}$  region: New excited levels in  $^{135}\text{Sb}$* , Phys. Rev. C **91**, 027303 (2015).

From this point on, the publications selected for the habilitation process will be referred to as H1, H2,..., H8, H9.

### 4.3 SCIENTIFIC MOTIVATION AND RESULTS FROM THE SELECTED PUBLICATIONS AND FUTURE PLANS.

#### 4.3.1 SCIENTIFIC MOTIVATION

The main goal of the cycle of publications that forms that basis of this habilitation is the study of properties of neutron-rich nuclei close to  $^{78}\text{Ni}$  and  $^{132}\text{Sn}$ , in particular to understand the evolution of single-particle levels in both regions.

Thanks to their simple structure, nuclei in the vicinity of double magicity attract large interest both from the experimental and the theoretical point of view. In order to describe them, it is possible to use the shell model with a closed core corresponding to the magic shells (see Figure 1, [1, 2]). Such nuclei have a spherical shape and the excitation-energy spectrum is dominated by single-particle excitations. The addition of nucleons beyond the closed shells leads to the polarisation of the core and appearance of deformation. The structure of such nuclei gets more complicated and difficult to describe within the shell model.

The majority of theoretical predictions uses experimental results in order to fit the key parameters for the models. The information most easily available concerns stable nuclei or nuclei in their close neighbourhood. In Figure 1 [1,2] the set of single-particle levels and magic numbers for nuclei at or close to the  $\beta$ -stability line is shown.

The advent of radioactive beams enabled a substantial shift of the available research areas towards exotic nuclei. In particular, it became possible to investigate experimentally the structure of neutron-rich nuclei, where the shell structure observed for stable nuclei can disappear and new energy gaps corresponding to new magic numbers can appear.

Different reasons exist for changes in the structure of very neutron-rich nuclei: changes in the depth and shape of the nuclear potential as well as the effect of the three-body force, which are described in details in the review papers of Refs. [3,4]. The theoretical investigations of the Tokyo group showed the important role of the monopole interaction between protons and neutrons occupying orbitals  $j_> = l + 1/2$  or  $j_< = l - 1/2$  [5, 6]. The strongest interaction is expected for the proton-neutron pair occupying orbitals with  $\Delta l=0$ , e.g.  $p_{3/2}-p_{1/2}$ ,  $d_{5/2}-d_{3/2}$ ,  $f_{7/2} - f_{5/2}$ ,  $g_{9/2} - g_{7/2}$ , and with  $\Delta l=1$ , e.g.  $p_{1/2} - d_{3/2}$ ,  $d_{3/2} - f_{5/2}$ ,  $f_{5/2} - g_{9/2}$ ,  $g_{7/2} - h_{11/2}$ .

The hypothesis of the disappearance of the N=8 shell was indeed experimentally verified for the isotope  $^{11}_3\text{Li}$ . In the case of  $^{11}\text{Li}$ , the phenomenon so-called *neutron halo*, which is associated with the distant spatial localisation of the weakly bound valence neutrons pair,  $S_{2n}$  is 369 keV with respect to the compact  $^9\text{Li}$  core. For this reason, the radius of  $^{11}\text{Li}$  is comparable with the radius of  $^{208}\text{Pb}$ . The investigation of neutron removal reactions showed that the measured momentum distribution of the neutron in  $^{11}\text{Li}$  can be reproduced by assuming a comparable

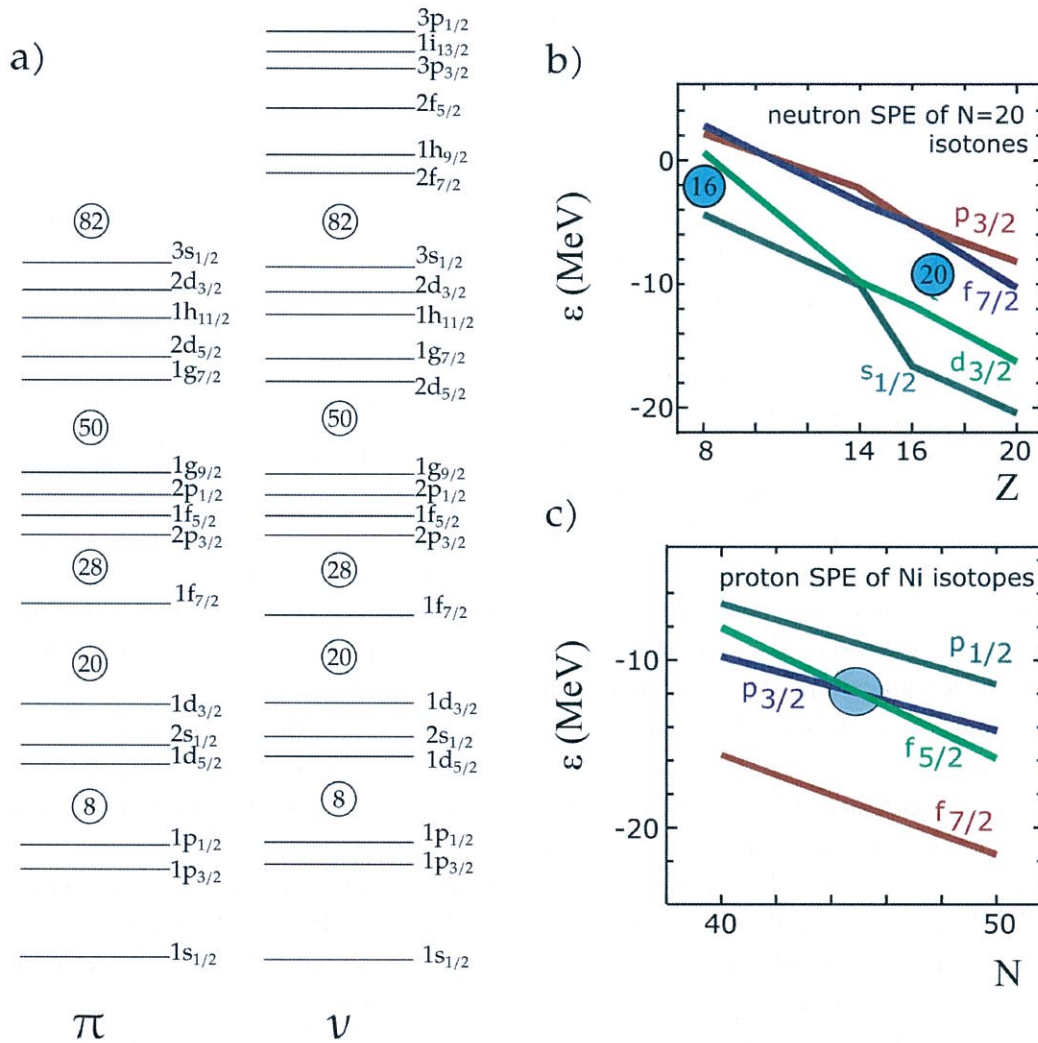


Figure 1: (a) Ordering of shell-model orbitals [1, 2] and their migration with the filling of (b) proton shells and (c) neutron shells [8].

filling of the orbitals  $p_{1/2}$  and  $s_{1/2}$  [7]. This shows that the neutron  $s_{1/2}$  orbital migrates through the  $N=8$  shell and the energy gap drops.

The evolution of the  $N=20$  shell as a function of the distance from the stability path was studied, by analyzing the excitation energy of the first  $2^+$  state in the  $N=20$  isotones. In the nuclei  ${}^{36}_{16}\text{S}_{20}$  and  ${}^{34}_{14}\text{Si}_{20}$  it reaches 3.3 MeV, while in the case of  ${}^{32}_{12}\text{Mg}_{20}$  drops to about 0.9 MeV.



This effect is associated with the decrease of the energy gap in the system of single particle states in  $^{32}\text{Mg}$ . Thanks to this, the mixing of states from higher shells ( $pf$ ) is possible, leading to deformation of the nucleus. The first  $2^+$  state becomes a collective state with low excitation energy and large matrix element for the  $2^+ \rightarrow 0^+$  transition. The evolution of single-particle states in the  $N=20$  isotones can be explained by considering the monopole interaction between protons filling the  $d_{5/2}$  orbital and neutrons in the  $d_{3/2}$ . As shown in Figure 1b, while decreasing the filling of the  $\pi d_{5/2}$  orbital, the  $\nu d_{3/2}$  orbital gets closer to the higher-lying  $\nu f_{7/2}$  orbital, causing the disappearance of the  $N=20$  shell and appearance of a new energy gap between the  $s_{1/2}$  and  $d_{3/2}$  orbitals. As a consequence, instead of  $N=20$ , the new  $N=16$  magic number appears. The predictions reported in Figure 1b found experimental validation. For example, the nuclei  $^{28}\text{O}$  and  $^{26}\text{O}$  are not bound, but a series of measurements of the momentum distribution in neutron removal reactions from the  $^{24}\text{O}$  projectile is well described under the assumption that the valence neutrons are occupying the  $s_{1/2}$  orbital [9]. The  $^{24}_8\text{O}_{16}$  isotope is therefore a doubly-magic spherical nucleus with new magic number  $N=16$ .

An analogous interaction to that for the  $\nu d_{3/2}$  and  $\pi d_{5/2}$  should be observed for the orbitals  $\nu f_{5/2}$  and  $\pi f_{7/2}$ . The effect of filling the  $\pi f_{5/2}$  orbital on the change of the position of the  $\nu f_{5/2}$  state can be investigated, e.g., by studying the properties of the  $N=34$  isotones starting from the stable  $^{62}_{28}\text{Ni}_{34}$  to  $^{54}_{20}\text{Ca}_{34}$ . The removal of the next protons from the  $\pi f_{7/2}$  orbital reduces the binding of the  $\pi f_{5/2}$  orbital. This leads to the formation of the subshell  $N=34$ , which is confirmed by the large values of the excitation energy of the  $2^+$  state in  $^{54}\text{Ca}$  (2 MeV) in comparison with the heavier  $N=34$  isotones, e.g. for  $^{56}\text{Ti}$   $E_{2^+}=1.1$  MeV [10].

The migration of single particle levels is predicted also in a heavier system like, e.g.,  $^{78}\text{Ni}$  (see Figure 1c) [5,6,8,11–14]. In this region of the chart of nuclei, the evolution of the proton orbitals above  $Z=28$  is generated by the filling of the neutron  $\nu g_{9/2}$  orbital (from  $N=41$  to  $N=50$ ). In this context the study of the properties of the ground- and excited states in Cu isotopes, which have only one proton outside the closed  $Z=28$  shell, is particularly interesting. The experimental results show that the excitation energy of the  $5/2^-$  state in Cu isotopes is almost constant at about 1 MeV. A clear change can be noticed for  $N \geq 42$  – the excitation energy of the  $5/2^-$  drops to 534 keV for  $^{71}\text{Cu}_{42}$  and 166 keV for  $^{73}\text{Cu}_{44}$ , respectively. This trend, predicted in the work of Ref. [8], indicates a change in the splitting of the proton orbits  $f_{5/2} - f_{7/2}$  and its reduction by about 2 MeV from  $N=40$  to  $N=50$ . This leads to the crossing of the proton orbitals  $f_{5/2}$  and  $p_{3/2}$  at  $N=46$  in the  $^{75}\text{Cu}$  [15–19]. From the beginning I have been involved in these works [16,17] and their continuation, with experiments in which I studied the  $\beta^-$  and  $\beta n$  decays of the next odd- $A$  copper isotopes [H1].

After crossing the  $N=50$  shell closure, the situation slightly changes when different neutron orbitals are filled. The size of the  $N=50$  energy gap depends on the proton-neutron interaction,

which between  $Z=28$  and  $Z=40$  corresponds to protons occupying the  $p_{3/2}$ ,  $f_{5/2}$  and  $p_{1/2}$  and neutrons above the closed  $N=50$  shell on the  $d_{5/2}$ ,  $g_{7/2}$ ,  $p_{3/2}$  and  $s_{1/2}$ . Independently on which of the proton orbitals, ( $\pi f_{5/2}$  or  $\pi p_{3/2}$ ) are occupied, the first valence neutron orbital will be  $\nu d_{5/2}$ . In the close neighbourhood of  ${}^{78}\text{Ni}$  the latter is expected to be degenerate with the neutron state  $\nu s_{1/2}$ . To date, the excitation energy of the  $1/2_1^+$  state in the light  $N=51$  isotones was not determined. For this reason in my work I focussed on the study of excited states in nuclei with one valence neutron lying above the doubly magic nucleus  ${}^{78}\text{Ni}$  and conducted a systematic study of the  $N=51$ ,  $N=52$  and  $N=53$  isotones to investigate the effect of additional neutrons on the structure of nuclei in this region [H2-H6]. Particular effort was put in the search for the single-particle neutron state  $s_{1/2}$  [H2-H3], for which in the heavier isotones a strong competition is generated by the configuration  $\nu d_{5/2} \otimes 2^+$ . The coupling of the neutron  $\nu d_{5/2}$  with the two protons ( $2^+$ ) gives us multiplets from  $1/2^+$  to  $7/2^+$ .

The study of the  $Z=50$  shell magicity comes down to understanding the evolution of the  $\pi g_{7/2}$  and  $\pi d_{5/2}$  proton orbitals. While filling the shell with neutrons, from  $N=50$  to  $N=82$ , a change in the spin of the ground state in odd  ${}_{51}\text{Sb}$  isotopes from  $I^\pi=5/2^+$  to  $7/2^+$  is observed between the two stable  ${}^{121}\text{Sb}$  and  ${}^{123}\text{Sb}$  [3]. This tendency is not preserved after the crossing of the magic neutron number  $N=82$ , where the energy of the first  $5/2^+$  state changes sharply from 963 keV in  ${}^{133}\text{Sb}$  to 282 keV in  ${}^{135}\text{Sb}$ . The research, in which I have been involved since the time of my doctoral studies, points to the possibility of a new migration of the  $\pi d_{5/2}$  and  $\pi g_{7/2}$ . For this reason, sometimes after the end of my PhD studies, I proposed to measure the lifetime of excited states in  ${}^{135}\text{Sb}$ , which allow to determine the wave function of both states [H7,H8]. This nucleus is very interesting also from the point of view of the search for the value of the energy of the single-particle state  $\nu i_{13/2}$  [H9]. The  $13/2^+$  level in  ${}^{133}\text{Sn}$  is expected to lie above the neutron separation energy. The addition of the extra proton and neutron to  ${}^{133}\text{Sn}$ , yielding  ${}^{135}\text{Sb}$ , allows to search for states associated to the neutron configuration  $\nu i_{13/2}$ .

The study of the evolution of single-particle states, interaction energies and  $\beta$ -decay properties, in particular the measurement of half-lives and  $\beta$ -delayed neutron emission probabilities  $P_n$ , are important not only for understanding the structure of exotic nuclei, but also they contribute to a better understanding of the observed abundances of the elements produced in the astrophysical r process. Its path on the chart of nuclei was predicted on the basis of the existing nuclear models. Therefore, their verification in the neutron-rich nuclei is extremely important. Our works confirm that new experimental results, like, e.g., the measurement of new half-lives of nuclei close to  ${}^{78}\text{Ni}$ , allow to constrain better the parameters of the models and have an impact on the results of the modelling of nucleosynthetic processes both in the  ${}^{78}\text{Ni}$  and  ${}^{132}\text{Sn}$  [20].

### 4.3.2 EXPERIMENTAL TECHNIQUES

The experiments which results are reported in publications H1-H9 were performed at three different laboratories, using different production methods and separation techniques. The technique to be used in the production/selection of the nuclei intense and therefore the laboratory where to perform the experiments, were selected so to have optimum production of the isotopes and beam quality (e.g. low-contaminant content in the secondary, radioactive, beam).

The isotopes of Ga, Ge, As and Cu [H1-H6] were produced in the proton-induced fission of  $^{238}\text{U}$  at the Holifield Radioactive Ion Beam facility (HRIBF) at Oak Ridge National Laboratory (ORNL), Oak Ridge, USA. The fission fragments diffused out of the target, were ionised, extracted from the ion source and accelerated to few tens of keV. At this point they were selected by means of two mass separators with resolution  $\Delta M/M=1/1000$  and  $1/10000$ , respectively. The isotopes selected through these stages were then directed to the centre of the experimental setup [H2].

An additional selection method was used for the production of clean radiative beams of Ge and As [H4-H6]:  $\text{H}_2\text{S}$  gas was added to the ion-source, where  $^A\text{Ge}$  and in part also  $^A\text{As}$ , ions formed the molecules  $^A\text{GeS}^{32+}$  and  $^A\text{AsS}^{32+}$ . Other (abundant) fission fragments like Br and Se, which belong to groups 16 and 17 of the periodic table, did not form such molecule. The first mass separator was set to accept ions with mass  $A+32$ . In this way isobars of mass  $A$  which did not form the molecule were removed from the radioactive beam. The beam was then direct to a charge-exchange cell in which the molecule was broken. The isotopes of interest,  $^A\text{Ge}$  and  $^A\text{As}$  were then analysed by the second (high-resolution) mass separator which accepted only isobars of mass  $A$ . The remaining contaminants at mass  $A+32$ , like the abundantly-produced Ag ions, were then removed from the beam.

As far as the isotopes of Cu are concerned, another innovative selection method was used [H1]. The fission fragments, selected according to their mass  $A$  through two-stage mass spectroscopy, were post-accelerated in the tandem accelerator at the HRIBF and directed to a micro-channel plate (MCP) detector and an ionization chamber (IC) filled with  $\text{CF}_4$  gas. The measurement of the energy loss of the ions along the IC allowed for the identification of the atomic number of the (monoenergetic) isobars on an event-by-event basis. Moreover, the IC allowed to remove the heavier and more abundant isobaric contaminants. With the exception of the isotopes with lowest  $Z$ , all other isotopes were stopped in the IC by increasing the pressure in the IC (ranging-out method). The measurements were done in two ways: ranging-out at a pressure of 200 Torr and pass-through at 100 Torr. The details of the two operation modes of the IC are given in the works [21–23].

Independently on the selection method adopted among those described above, the radioactive beam was implanted on a tape positioned in the centre of the detection set-up. The latter

consisted in two scintillation detector for  $\beta$  counting and an array of four clover detectors to register  $\gamma$  rays. The radioactive beam was periodically deflected away by means of an electrostatic deflector placed upstream from the implantation point. The time structure of the beam on the tape therefore consisted of two intervals: *beam-on* during which the beam was implanted onto the tape and *beam-off* when the beam was deflected away. At the end of the latter time the tape was moved to remove the long-lived daughter activity from the measuring point. Data on the decay of the isotopes of interest were collected during both the beam-on (grow-in of activity) and beam-off (decay) phases. The duration of each such time interval was determined and optimized for each of the isotopes individually on the basis of their respective half-lives. The data were collected using trigger-free digital electronics.

The neutron-rich nuclei investigated in the works described in the publications [H7] and [H8] were produced in neutron-induced fission of  $^{238}\text{U}$  and separated by a standard on-line mass separator. The experiments were conducted at the Studsvik OSIRIS separator in Sweden. Their goal was the identification of excited states in  $^{135}\text{Sb}$  populated in  $\beta$  decay of  $^{135}\text{Sn}$ . Also in this case a tape transport system was used to remove unwanted long-lived background and daughter activity. The main difference in the detection set-up with respect to that described above is the use of fast scintillation detectors for gamma-ray detection. This detectors system allowed to measure the lifetime of excited states in the isotopes studied. The technique consists in the measurement of triple coincidences using different detectors (fast  $\beta$  and  $\gamma$  scintillators and germanium detectors) and very precise time calibration [24–26]. The principle of the experiment is similar to the use of a stop watch. The  $\beta$  detector starts the direct measurement of time and the fast scintillator stops it. The germanium detector does not directly take part in the time measurement but, when more decay branches are available, selects the  $\gamma$  cascade chosen for the fast detectors. The precision of such technique is incredible good, of the order of 3 ps.

High-spin states cannot be observed when studying low-spin states populated in  $\beta$  decay. Complementary information can be obtained by studying the  $\gamma$  decay of excited states populated in spontaneous fission using the multi-detector germanium array EUROGAM2 [27] [H9]. The geometry of the system allows in this case to study angular correlations of the gamma radiation, and therefore deduce the multipolarity of the transitions.

### 4.3.3 RESULTS

#### DECAY PROPERTIES OF NUCLEI CLOSE TO $^{78}\text{Ni}$

In order to study the evolution of single-particle proton levels in neutron-rich nuclei it is necessary to select nuclei that are characterised by a simple structure. In this respect, nuclei in the region close to the doubly-magic nucleus  $^{78}\text{Ni}$  are particularly interesting. For example,

the study of  $\beta$  decay of the isotopes  $^{69}\text{Cu}_{40}$ – $^{79}\text{Cu}_{50}$ , which have only one valence proton outside the closed  $Z=28$  shell, allowed to track the evolution of proton states while filling the  $\nu g_{9/2}$  ( $N=40$ – $50$ ) shell. In particular, the crossing of the  $\pi f_{5/2}$  and  $\pi p_{3/2}$  between  $^{75}\text{Cu}$  and  $^{77}\text{Cu}$  was identified. This is a consequence of the splitting of the  $\pi f_{5/2}$ – $\pi f_{3/2}$  and  $\pi p_{3/2}$ – $\pi p_{1/2}$  orbitals [16, 17].

The study of neutron-rich Cu isotopes was extended to the next two isotopes  $^{78,79}\text{Cu}$ , as reported in publication [H1]. The absolute feedings of excited states in the daughter nucleus were determined as well as and their spin and parity. For the first time it was possible to determine the spin of the ground state of  $^{78}\text{Cu}$  ( $5^-$ ) and to observe the  $\beta$ -delayed neutron  $\gamma$  decay of  $^{79}\text{Cu}$  to the first  $2^+$  state in  $^{78}\text{Zn}$ . Moreover, I performed the theoretical calculations which, together with the experimental probabilities for  $\beta n$  emission ( $P_n$ ), confirm the spin and parity  $I^\pi=5/2^-$  for the ground states of  $^{77,79}\text{Cu}$ , as reported in publication [H1]. After the shell closure at  $N=50$  the evolution of the structure of the nuclei may vary, since other neutron states play a role. Here the valence neutrons fill the neutron orbitals:  $1g_{7/2}$ ,  $2d_{5/2}$ ,  $3s_{1/2}$ ,  $1h_{11/2}$ ,  $2d_{3/2}$  (see Figure 1a). With the increase of neutrons beyond the magic  $N=50$  number, it is predicted that, a part from the crossing of the  $\pi f_{5/2}$  and  $\pi p_{3/2}$  orbitals, the  $\nu d_{5/2}$  and  $\nu s_{1/2}$  are degenerate [28]. Theoretical calculations suggest that the addition of a few valence nucleons to the closed  $^{78}\text{Ni}$  core causes a fast inset of deformation. This was observed already in  $^{86}\text{Ge}$  and  $^{88}\text{Se}$  [29]. Mean field Hartree-Fock-Bogoliubov calculations with Gogny force point to shape coexistence in this region [30].

In order to validate different theoretical calculations, experimental information for isotopes that have a simple structure, i.e. one, two or three valence neutrons outside the closed core, needs to be collected. For this reason I proposed to study the  $\beta$  decay of the neutron-rich  $^{85}\text{Ga}$  nucleus, measurement which led to the identification of several new excited states in  $^{85}\text{Ge}_{53}$  and  $^{84}\text{Ge}_{52}$  [H2]. The continuation of this work was the study of the  $\beta$  decay of  $^{84,85}\text{Ge}$  and  $^{87}\text{As}$  [H4,H5,H6]. The new experimental data allowed to complement the existing knowledge on the evolution of the structure for  $N=51$ , 52 and 53 isotones. The study of the  $\beta$  decay of  $^{84}\text{Ge}$  described in the publication [H4] allowed to identify several new excited states in the daughter  $^{84}\text{As}$  and pointed to the necessity of changing the sequence of three previously known levels in this nucleus. Particular attention should be paid to the feeding of two states above 2.5 MeV in the  $\beta$  decay of  $^{84}\text{Ge}$ . These, according to shell model calculations, correspond to the  $\beta$  decay of a neutron from the  $\nu d_{5/2}$  orbital into a proton on the  $\pi f_{5/2}$  orbital. On the basis of the  $\beta$  intensities for these levels (upper limits for the absolute intensity), the  $\log ft$  value for the observed  $\beta$  transition was calculated ( $\log ft > 4.6$ ). The values suggested allowed Gamow-Teller character for these transitions and permitted to assign  $I^\pi=1^+$  to the two levels. The location of the

two  $1^+$  states identified in  $^{84}\text{As}$  is consistent with the systematics of  $I^\pi=1^+$  states in the  $N=51$  isotone chain (see Figure 2).

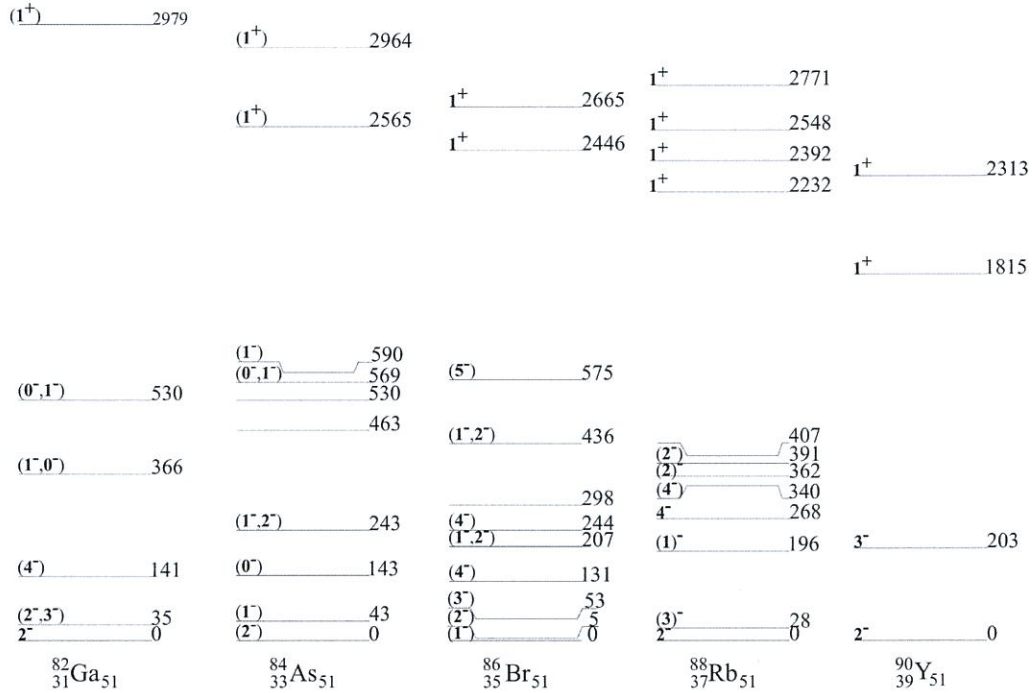


Figure 2: Systematics of low-spin excited states in the  $N=51$  isotones [34–37], [H4]. Level energies are in keV. Two different scales are used for states below and above 1 MeV for clarity.

Low-lying levels in  $^{84}\text{As}$  with excitation energy below 0.5 MeV are fed by first forbidden transitions due to the transformation of a neutron from the  $\nu d_{5/2}$  or  $\nu s_{1/2}$  orbital into a proton on the  $\pi f_{5/2}$  or  $\pi p_{3/2}$  orbital. Theoretical calculations that I performed in the framework of the shell model (SM) using the Nushellx code [31] with N3LO interaction [32–34] support this interpretation and well reproduce the layout of the levels in  $^{84}\text{As}$ . The calculations show that low-lying excited states in  $^{84}\text{As}$  are formed by a neutron on the  $\nu d_{5/2}$  or  $\nu s_{1/2}$  orbital coupled to a  $\pi f_{5/2}$  or  $\pi p_{3/2}$  proton.

The investigation of excited states in the  $N=52$  isotone chain allows to study the evolution of single-particle proton states. The results of the measurement of the  $\beta$  decay of  $^{85}\text{Ge}$  populating levels in  $^{85}\text{Ge}_{52}$  are presented in publication [H5]. The analysis of the experimental data for this isotope was conducted in the framework of a master thesis conducted under my supervision. Several previously-unobserved transitions in  $^{85}\text{As}$  were identified and for the first time a partial decay scheme of  $^{85}\text{Ge}$  was constructed. Spin and parity  $I^\pi=(5/2^-)$ ,  $(3/2^-)$  and

$(1/2)^-$  were proposed for the ground state and first two excited states in  $^{85}\text{As}$ , respectively, see Figure 3. This was based on the intensities for the  $\beta$  transition in the decay of the  $I^\pi=(3/2)^+$  ground state of  $^{85}\text{Ge}$  and on the existing systematics of low-lying states in the  $N=52$  isotones  $^{86}\text{Ga}$  [23] and  $^{87}\text{Br}$ .

In this context I performed shell model calculations using the Nushell code [31] with N3LO interaction [32, 33] and including all active orbitals outside the closed  $^{78}\text{Ni}$  core. They are reported in publication [H5] and shown in Figure 3.

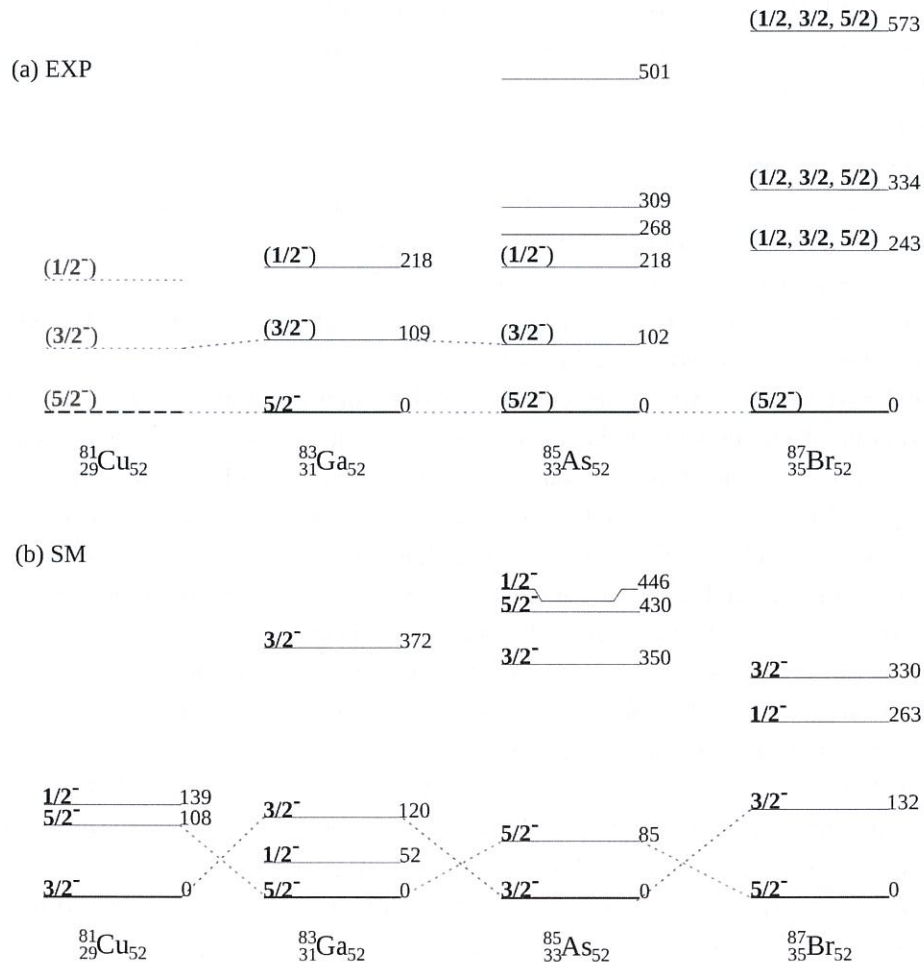


Figure 3: Systematics of low-spin excited states in the  $N=52$  isotones from experiment (solid lines) [H5] and prediction for  $^{81}\text{Cu}$  based on the systematic of the heavier isotones (dotted lines), [34, 37]. Level energies are in keV.

The number of predicted excited states in  $^{83}\text{Ga}$ ,  $^{85}\text{As}$  and  $^{87}\text{Br}$  is in agreement with the experimental data, although their ordering is within the uncertainty limits of the model (200-300 keV). In the low excitation-energy region the calculations predict only the presence of negative-parity states. In the decay of the  $I^\pi=(3/2^+)$   $^{85}\text{Ge}$  ground state they can be fed only by forbidden transitions. This is confirmed by the  $\log(ft)$  values reported in publication [H5].

The theoretical calculations showed that the wave function of the lowest-lying  $5/2^-$ ,  $3/2^-$  and  $1/2^-$  states in  $^{87}\text{Br}$ ,  $^{85}\text{As}$  and  $^{83}\text{Ga}$  is dominated (70-80%) by neutrons in the  $\nu d_{5/2}$  orbital, with the contribution of neutrons in the  $\nu s_{1/2}$  orbital not larger than 20%. The proton wave function of  $^{87}\text{Br}$ ,  $^{85}\text{As}$  and  $^{83}\text{Ga}$  is more complex, with 40-to-50% of contribution from the orbitals  $\pi f_{5/2}$  and  $\pi p_{3/2}$ . However, the calculations I performed showed that the structure of low-lying excited states in  $^{82}\text{Cu}_{52}$  is defined by the properties of the valence proton, in agreement with expectations. In the ground-state it can occupy the  $\pi p_{3/2}$  or  $\pi f_{5/2}$  orbital and its contribution to the wave function amounts to 80%. The extrapolation of the systematics of low-lying excited states in the N=52 isotones to  $^{81}\text{Cu}$  suggests spin and parity  $5/2^-$  for its ground state. The calculations predict also inverse sequence of the  $5/2^-$  and  $3/2^-$  states. The verification of these predictions can be achieved only after gathering experimental information on the spin and parity of low-lying excited states in  $^{81}\text{Cu}$ .

In the N=51 isotones, which are characterised by one neutron outside the closed N=50 shell, the dominant component of the wave function is constrained by next single-particle orbitals  $\nu d_{5/2}$  and  $\nu s_{1/2}$ . Therefore, the spin and parity for the ground state of N=51 isotones are  $5/2^+$  ( $\nu d_{5/2}$ ) and for the first excited states  $1/2^+$  ( $\nu s_{1/2}$ ). On the other hand, the properties of the neutron states in the N=53 isotones are different from those of states in nuclei with N=51. The two additional neutrons on the  $\nu d_{5/2}$  orbital generate the appearance of a low-lying  $3/2^+$  state. Such state was observed in the N=53 isotones  $^{97}\text{Ru}$ – $^{91}\text{Sr}$ , in which the spin and parity of the ground state are  $5/2^+$  and the first excited state has  $3/2^+$ . In the  $^{89}\text{Kr}_{53}$  nucleus the order of the  $5/2^+$  and  $3/2^+$  states is inverted and  $3/2^+$  is the ground state. In the publications [H9, H5, H6] the study of the  $\beta$  decays  $^{87}\text{As}\rightarrow^{87}\text{Se}$  [H9] and  $^{85}\text{Ga}\rightarrow^{85}\text{Ge}$  [H5, H6] showed that such ordering of the  $3/2^+$  and  $5/2^+$  states is preserved in  $^{87}\text{Se}$  and  $^{85}\text{Ge}$  (see Figure 4). This investigation of  $^{87}\text{As}$  and  $^{85}\text{Ga}$  did not allow for the identification of the  $1/2^+$  state, which is associated with the excitation of the single-particle state  $\nu s_{1/2}$ , since this level is poorly fed in the  $\beta$  decay of the ground state of  $^{87}\text{As}$  and  $^{85}\text{Ga}$  which have spin and parity  $5/2^-$ . The  $1/2^+$  state in  $^{85}\text{Ge}$  was identified in the study of the  $\beta n$  decay of  $^{86}\text{Ga}$  [38] and it can be expected that the  $1/2^+$  state in  $^{85}\text{Ge}$  should be observed in the  $\beta n$  decay of  $^{88}\text{As}$ . Within the framework of the shell model, I performed some calculations on the structure of low-lying excited states of the N=53 isotones  $^{87}\text{Se}$ ,  $^{85}\text{Ge}$  i  $^{83}\text{Zn}$ , which are reported in publication [H5]. As shown in Figure 4, the calculations correctly reproduce the observed  $3/2^+$  and  $5/2^+$  states in  $^{87}\text{Se}$



and  $^{85}\text{Ge}$ . The wave functions of these states are admixed. The structure of the  $5/2^+$  state is defined mainly (55-60%) by the coupling of  $(\nu d_{5/2}^3)$   $5/2^+$  with the  $0^+$  proton state and by 20-25% by coupling of the  $(\nu d_{5/2}^3)$   $3/2^+$  with the proton excitation  $2^+$ . The  $3/2^+$  states are result of the coupling of  $(\nu d_{5/2}^3)$   $3/2^+$  with the proton state  $0^+$  (45-50%) with significant contribution (25-35%) of  $(\nu d_{5/2}^3)$   $5/2^+$  coupled to proton excitation  $2^+$ . The lowest-lying  $1/2^+$  state has single-particle character and is due to the unpaired neutron sitting on the  $s_{1/2}$  orbital. On the basis of systematics of experimental data and theoretical calculation I proposed a possible level scheme for excited states in the lightest N=53 isotope  $^{83}\text{Zn}$  (see Figure 4). Similarly to the situation in  $^{85}\text{Ge}$  and  $^{87}\text{Se}$ , the lowest-lying states are  $5/2^+$ ,  $3/2^+$  and  $1/2^+$ .

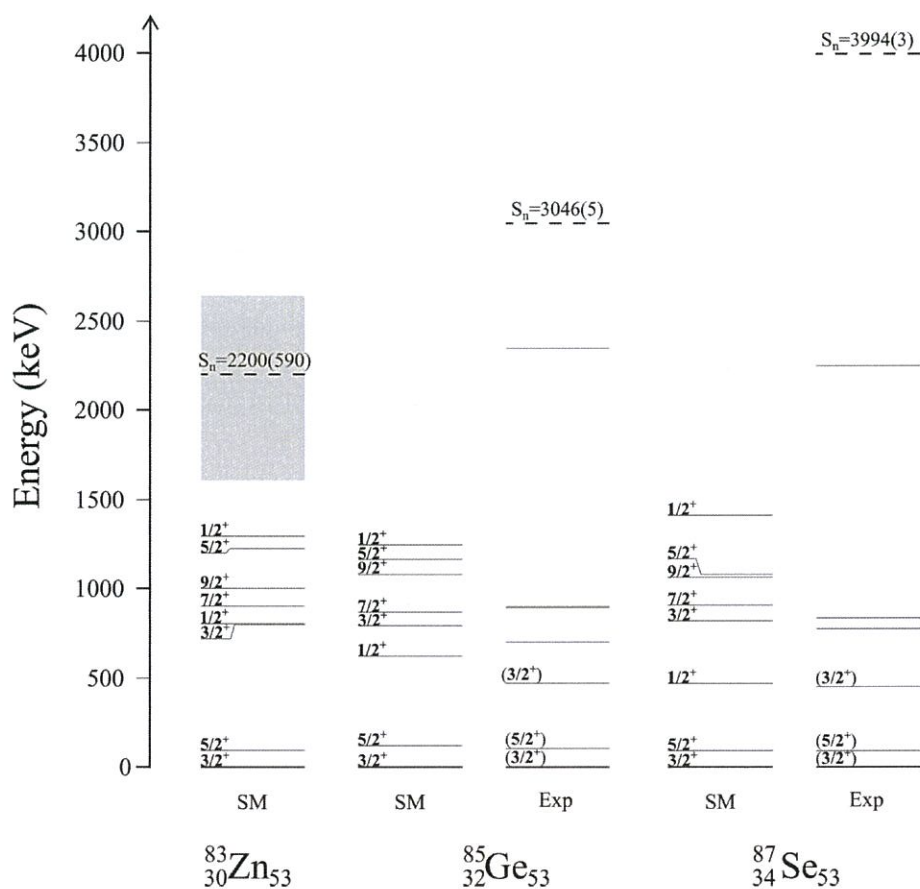


Figure 4: Systematics of low-spin excited states in the N=53 isotones from experiment and from shell model calculations [37], [H6]. Level energies are in keV.

These can be fed directly by first-forbidden transitions in the  $\beta$  decay of  $^{83}\text{Cu}$  or in the allowed decay of  $^{84}\text{Cu}$  followed by neutron emission.

The new spectroscopic data obtained for the N=52, 52 and 53 isotones are important in order to understand the structure of so neutron-rich isotopes. These are nuclei close to the doubly-magic nucleus  $^{78}\text{Ni}$  and yet, an increase of collectivity for the N=52 and 53 isotones was observed as the proton number increases [38, 39]. The experimental knowledge of the spin values is one of the crucial pieces of information in order to determine unambiguously the nature of these states. To date, the majority of the spin/parity was deduced/proposed on the basis of the values of the *logft* observed in the  $\beta$  decay and of the systematics of levels in the neighbourhood. Precise information on the structure of excited states can be obtained through their lifetime measurement. In this context I proposed an experiment at the ALTO facility in Orsay, Paris, to measure the lifetime of excited states in the isotopes  $^{81}\text{Ge}_{49}$ ,  $^{83}\text{Ge}_{51}$  and  $^{85}\text{Ge}_{53}$ .

#### STUDY OF STRUCTURE OF NUCLEI IN THE NEIGHBOURHOOD OF $^{132}\text{Sn}$

One of the interesting results of my doctoral thesis was the measurement of the low-lying excited state in the nucleus  $^{135}_{51}\text{Sb}_{84}$ ,  $E^*=282$  keV, to which spin  $I^\pi=(5/2^+)$  was assigned, while the excitation energy of the analogue state in  $^{133}_{51}\text{Sn}_{82}$ , which corresponds to the proton single-particle state  $\pi d_{5/2}$ , is 962 keV [40]. The significant decrease in energy of this state in the  $^{135}\text{Sb}$  isotope, which has only two neutrons more than  $^{133}\text{Sb}$ , was explained as a shift in the single-particle energy or migration of the levels as effect of the  $l \cdot s$  splitting [8].

In order to determine the experimental value of the spin for the level  $E^*=282$  keV, after the completion of the doctoral studies, I proposed an experiment at the Studsvik laboratory, with the goal of measuring the lifetimes of the excited states in  $^{135}\text{Sb}$  populated in the  $\beta$  decay of  $^{135}\text{Sn}$  [H7,H8]. The experiment was performed using the so-called *time-delay*  $\beta\gamma\gamma$  method for determining lifetimes [24].

The strong feeding of the  $E^*=282$  keV state in  $^{135}\text{Sb}$  populated in the  $\beta$  decay of the  $^{135}\text{Sn}$  ground state [41] points to a dominant single-particle  $\pi d_{5/2}$  component in this state, in analogy to what observed in  $^{133}\text{Sb}$  [42]. An M1 transition is forbidden between single-particle  $d_{5/2}$  and  $g_{7/2}$  states, whereas E2 collectivity is small in this region. As a consequence, it should be possible to observe in  $^{135}\text{Sb}$  a transition with  $E_\gamma=282$  keV and very slow B(M1), if the shift of the single-particle orbital is observed, or a fast transition in case the decrease of excitation energy of the excited state is due to collectivity. Upper limits for  $B(\text{M1}) \leq 0.30 \cdot 10^{-3} \mu_N^2$  and  $B(\text{E2}) \leq 54 \text{ e}^2\text{fm}^4$  (see Figure 5) were set on the basis of the measured lifetime  $T_{1/2}=6.1(4)$  ns. By comparing the experimental value with theoretical calculations presented in the publication [H7], we confirmed the dominant component to be  $\pi d_{5/2}$  for the  $E^*=282$  keV state in  $^{135}\text{Sb}$ .

Analogue properties are observed for  $^{211}\text{Bi}$ , which is the complementary isotope in the  $^{208}\text{Pb}$  region (see Figure 5), confirming the analogies of the  $^{132}\text{Sn}$  and  $^{208}\text{Pb}$  regions [43].

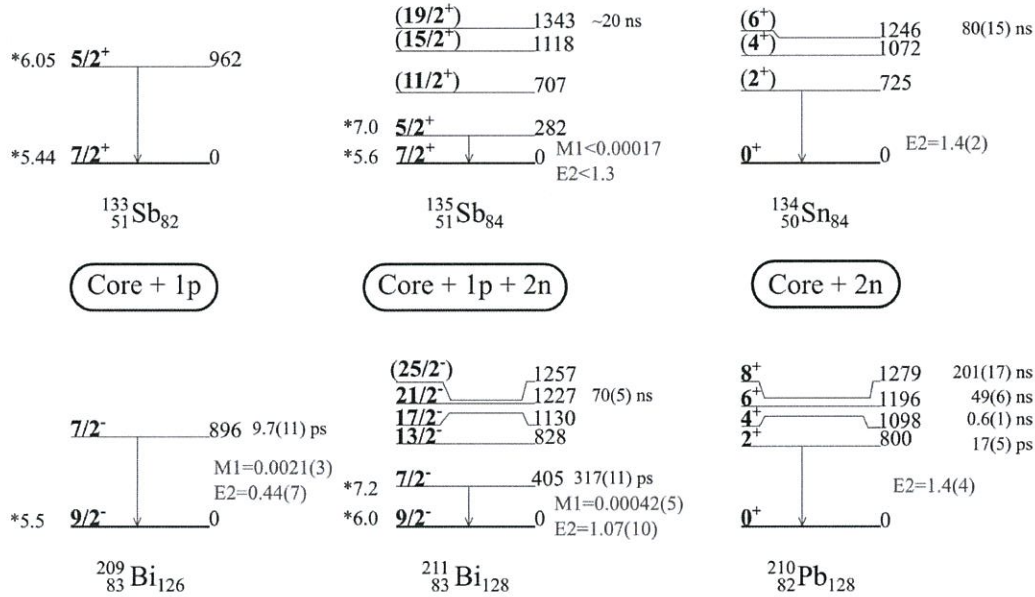


Figure 5: Partial level scheme of the isotopes in the  $^{132}\text{Sn}$  region (upper portion of the figure) and of the complementary isotopes in the region of  $^{208}\text{Pb}$  (lower portion of the figure) [H7, H8], [37].

Another open question in the  $^{132}\text{Sn}$  region is the energy of the  $\nu i_{13/2}$  single-particle. The situation in this case is particularly complicated, since its predicted value places it above the neutron separation energy ( $S_n$ ) in  $^{133}\text{Sn}$  [44]. The first estimate of this energy, 2700(200) keV [45], based on the excitation energy of the  $I^\pi = 10^+$  level in  $^{134}\text{Sb}$  (configuration  $\pi g_{7/2} \nu i_{13/2}$ ) suffered from large uncertainties. Unfortunately, its energy was known only with respect to the isomeric state  $I^\pi = 7^-$  in  $^{134}\text{Sb}$ , which is reflected in the large uncertainty of the value determined. Over the last 20 years several measurements were carried on in this region, which allowed to constrain the energy of the  $7^-$  isomeric state to good precision ( $E^* = 279(1)$  keV [46]), but no better value was proposed for the long searched single particle energy.

In my work I tried to determine the energy of the  $\nu i_{13/2}$  single-particle state. In order to achieve this not only is the known excitation energy of the  $I^\pi = 10^+$  level needed, but also the knowledge of the interaction energy of the valence nucleons  $\pi g_{7/2} \nu i_{13/2}$ . Unfortunately, such energy is not known with sufficient precision in this region. Nevertheless, it is possible to constrain its value by scaling the energy of the corresponding interaction in the  $^{208}\text{Pb}$  region

[43] taking into account the mass correction  $A^{-1/3}$ . The complementarity of the two regions [43] shows that the states with quantum numbers  $n, l, j$  in the  $^{132}\text{Sn}$  region correspond to states with quantum numbers  $n, l+1, j+1$  in the  $^{208}\text{Pb}$  region. The calculations led to an interaction energy for  $\pi g_{7/2}\nu i_{13/2}$  of  $V_1^{10+} = -723$  keV. In order to reduce the uncertainty on this quantity, a similar scaling was done for a few selected configurations. Their value  $V_1$  was compared with the interactions  $V_2$  calculated in the  $^{132}\text{Sn}$  region and the difference  $\Delta V = V_2 - V_1$  is shown in the last column of Table 1. The maximum discrepancy is about 70 keV and such value was assigned to the uncertainty for the interaction energy of interest ( $V_1^{10+} = -723(70)$  keV)

Table 1: Interaction energies  $V_0, V_1$  and  $V_2$  between valence nucleons beyond the doubly magic cores  $^{208}\text{Pb}$  and  $^{132}\text{Sn}$ . The symbol  $V_2$  indicates the interaction calculated in the  $^{132}\text{Sn}$  region,  $V_0$  the interaction in the  $^{208}\text{Pb}$  region, and  $V_1$  after scaling by the mass coefficient in the  $^{132}\text{Sn}$  region. The difference between the calculations in a given region and the scaled interaction is shown in the last column  $\Delta V = V_2 - V_1$ . All values are in keV.

$^{208}\text{Pb} \rightarrow ^{132}\text{Sn}$			$^{132}\text{Sn}$		
configuration	$V_0$	$V_1$	configuration	$V_2$	$\Delta V$
$(\pi h_{9/2}\nu j_{15/2})_{12+}$	-621	-723	$(\pi g_{7/2}\nu i_{13/2})_{10+}$		
$(\pi h_{9/2}\nu g_{9/2})_{9-}$	-396	-461	$(\pi g_{7/2}\nu f_{7/2})_{7-}$	-488	-27
$(\pi h_{9/2}\nu i_{11/2})_{10-}$	-776	-903	$(\pi g_{7/2}\nu h_{9/2})_{8-}$	-976	-73
$(\pi i_{13/2}\nu g_{9/2})_{11+}$	-960	-1117	$(\pi h_{11/2}\nu f_{7/2})_{9+}$	-1154	-37
$(\nu g_{9/2}\nu i_{11/2})_{10+}$	-221	-257	$(\nu f_{7/2}\nu h_{9/2})_{8+}$	-280	-23
$(\pi h_{9/2}\pi f_{7/2})_{8+}$	+107	+125	$(\pi g_{7/2}\pi d_{5/2})_{6+}$	+201	+76

In additional calculations the state of maximum spin set  $(\pi g_{7/2}\nu i_{13/2})_{10+}$  was depicted by describing its excitation energy as the sum of the energies of the single particle  $\pi g_{7/2}$  and  $\nu i_{13/2}$  and the interaction energy between them [47]. The value of the mass deficit used in the calculations was taken from Refs. [48, 49]. The new result  $\epsilon_{\nu i_{13/2}} = 2669(70)$  keV is close to the previous value 2694(200) keV, but has three times smaller uncertainty.

The value determined is larger than the neutron separation energy  $S_n = 2400$  keV in  $^{133}\text{Sn}$  [44], while in the heavier  $N=83$  isotones  $^{135}\text{Te}$  and  $^{137}\text{Xe}$  the neutron levels on the  $\nu i_{13/2}$  are bound. An interesting question is how much above the  $S_n$  we can expect the  $13/2^+$  level in  $^{133}\text{Sn}$  and whether it is possible to observe it experimentally. For the  $N=83$  isotones we expect two excited levels with spin  $13/2^+$ , which can mix their configurations: one with single-particle nature  $\nu i_{13/2}$  and the second one with octupole excitation built on the ground state  $(3^- \times \nu f_{7/2+})_{13/2+}$ . The systematics of excitation energies of states with spin  $13^+$  in the  $N=83$  isotones and the position of the octupole excitation in the  $N=82$  core are shown in publication [H9]. The analysis of the systematic trend and the knowledge of the octupole excitation energy

in  $^{132}\text{Sn}$  (4352 keV) allowed to calculate the excitation energy of the lower-lying  $13/2^+$  state in  $^{133}\text{Sn}$ . The value obtained, 2511(80) keV, shows that this state is unbound with respect to neutron emission. Its excitation energy is so close to the  $S_n$  that the de-excitation of the  $13/2^+$  state by emission of  $\gamma$  radiation is possible. In our analysis we limited ourselves to single-particle states and the possible octupole excitations, since such is the nature of states in  $^{209}\text{Pb}$ . A similar approach which took also into account quadrupole excitations, allowed the authors of Ref. [50] to delimit the position of the  $\nu i_{13/2}$  state in the range  $2360 \text{ keV} \leq \epsilon_{\nu i_{13/2}} \leq 2600 \text{ keV}$ . In order to verify experimentally these predictions, I proposed an experiment at the facility ISOLDE at CERN to study excited states in  $^{133}\text{Sn}$ . These states were populated in the  $\beta^-$  decay of the  $I^\pi=9/2^-$  ground state and of the  $I^\pi=1/2^-$  isomer of  $^{133}\text{In}$ . Thanks to the use of the laser ion source coupled to mass separation, the separation of the ions in the isomeric state from those in the ground state was possible and their decays can be studied independently. In the same experiment the  $\beta^-$  and  $\beta n$  decay of  $I^\pi=(3-7)^-$   $^{134}\text{In}$  were investigated. The data collected are being analysed in the framework of a PhD thesis under my supervision.

#### 4.3.4 SUMMARY AND OUTLOOK ON FUTURE RESEARCH

The advent of radioactive beam facilities produced a great potential for experiments conducted with the use of such beams. An example of such possibilities offered e.g. by the laboratory RIKEN in Japan, is the results of an experiment conducted not long ago to which I participated. During it the  $\beta n$  decay of several very neutron-rich nuclei using a  $^3\text{He}$  counter was studied. For the first time it was possible to observe the decay of extremely exotic nuclei such as  $^{84}\text{Cu}$  and  $^{140}\text{Sn}$ . The research in which I was engaged over the last several years allowed to study, among others, the structure of the  $N=51$ ,  $52$  and  $53$  isotones close to the doubly magic  $^{78}\text{Ni}$  and of nuclei close to  $^{132}\text{Sn}$ , allowing to gather information on the single-particle states  $\nu d_{5/2}$  and  $\nu i_{13/2}$ . Unfortunately not all questions could be answered. In particular, information on the energy of the  $\nu s_{1/2}$  orbital in the  $^{78}\text{Ni}$  region and  $\nu i_{13/2}$  close to  $^{133}\text{Sn}$  is still missing. The reasons for this are the low production rate of such exotic nuclei, the weak feeding in  $\beta$  decay of the states of interest and the non-sufficient efficiency of the detection systems. I plan to continue such research under much better experimental conditions. I submitted a proposal to measure the lifetime of excited states in  $^{81}\text{Ge}_{49}$ ,  $^{83}\text{Ge}_{51}$  and  $^{85}\text{Ge}_{53}$ , which was accepted by the Program Advisory committee of the facility ALTO at IPN Orsay, France. The experiment is planned in autumn 2017. At the facility ALTO I also plan to conduct an experiment that has the possibility to observe the  $\nu s_{1/2}$  orbital in another nucleus close to  $^{78}\text{Ni}$ , namely  $^{87}\text{Se}$ . In this case, instead of looking directly for the  $1/2^+$  state in the forbidden decay of  $^{87}\text{As}$  ( $I_{g.s.}^\pi=(3/2^-)$ ), we will study the  $\beta n$  decay of  $^{88}\text{As}$  to  $^{87}\text{Se}$ , which can feed the  $1/2^+$  state. Such approach was

instrumental to observation of the  $\nu s_{1/2}$  orbital in  $^{85}\text{Ge}$  – this state was not observed in the  $\beta\gamma$  decay of  $^{85}\text{Ga}$  [H2], but was observed in the  $\beta^-$  decay of  $^{86}\text{Ga}$  [38].

Following the studies in the neighbourhood of  $^{132}\text{Sn}$ , I proposed an experiment at CERN-ISOLDE with the purpose of measuring single-particle states in  $^{133}\text{Sn}$  populated in the  $\beta$  decay of  $^{133}\text{In}$  ( $I_{g.s.}^\pi=9/2^-$ ),  $^{133m}\text{In}$  ( $I_m^\pi=1/2^-$ ) and in the  $\beta n$  decay of  $^{134}\text{In}$  ( $I_{g.s.}^\pi=4^- - 7^-$ ). The two  $^{133}\text{In}$   $\beta$ -decaying states populate different groups of levels in the  $^{133}\text{Sn}$  daughter. Thanks to the possibility of applying selective separation for ions in the ground- and in isomeric-states using a laser ion-source, it is possible to study the two decays independently. The preliminary analysis of the data collected in the experiment is extremely promising and indicates, for example, the unexpected presence of several new  $\gamma$  transitions originating well above the neutron separation energy in  $^{133}\text{Sn}$ . The data will form part of a PhD thesis under my direct supervision. Because of the large probability for emission of neutrons for  $^{133}\text{In}$  and  $^{134}\text{In}$ , the measurement of the energy of the delayed neutrons is important. Such experiment was performed in May 2017 at CERN ISOLDE using the neutron spectrometer VANDLE (*Versatile Array for Neutron Detection at Low Energies*), to which I took part. The next step in this research will be to propose measurements using a total absorption spectrometer for  $\gamma$  radiation (TAS). This kind of detector is characterised by very high efficiency for  $\gamma$  radiation (90%), making it an extremely powerful tool when registering high-energy  $\gamma$  rays, as is the case in the decay of nuclei close to  $^{132}\text{Sn}$ .

At present, the majority of the leading facilities in this field has programs for the construction of the next generation of laboratories, in order to improve the current production rates by 2-to-4 orders of magnitude. The largest new laboratories under construction are the Facility for Rare Isotope Beams (FRIB) in USA, the Facility for Antiproton and Ion Research (FAIR) in Germany, Système de Production d'Ions Radioactifs Accélérés en Ligne (SPIRAL2) in France and the High Intensity and Energy (HIE)-ISOLDE in Switzerland. Significant progress can be expected in a number of research areas that make use of radioactive beams: from nuclear structure and reactions to the physics of nucleosynthesis and of fundamental interactions.

## 5 OTHER SCIENTIFIC INTERESTS

The main scope of my research interests is the understanding of the structure of nuclei far from the  $\beta$  stability valley. One of the fundamental difficulties that hinders this kind of research is the limited possibility to produce and separate nuclei with large excess of neutrons or protons. The extension of the investigations towards the so-called *terra incognita* is strongly bound to the development of new experimental techniques and tools. Nowadays, real pioneering research can be carried out only in few research centres in the World, like those in which exotic radioactive beams are produced. Still, the most interesting nuclei from the point of view of nuclear structure and of the astrophysical processes remain at the edge of the capabilities of present day facilities. My interests in exotic nuclei are not limited to one region of the chart of nuclei. Thanks to the employment of different experimental techniques, I am involved in studies of nuclei with number of protons (and/or neutrons) close to magic numbers ( $^{132}\text{Sn}$ ,  $^{100}\text{Sn}$ ,  $^{78}\text{Ni}$ ,  $^{68}\text{Ni}$ ) and of extremely exotic nuclei close to the proton- ( $^{45}\text{Fe}$ ) and neutron- ( $^8\text{He}$ ) drip-lines.

### 5.1 SCIENTIFIC INTERESTS DURING THE STUDIES

#### 5.1.1 MASTER STUDIES

During my master thesis work I focused on the study of isomeric states in the isotopes  $^{69}\text{Ni}$  and  $^{71}\text{Cu}$ , which are particularly interesting for their vicinity to the closed  $Z=28$  shell and  $N=40$  sub-shell. The results of the experiment, which was conducted at the GANIL laboratory in France, was the production and identification of seventeen new isomeric states produced in the fragmentation reaction of  $^{86}\text{Kr}$  on a  $^{nat}\text{Ni}$  target [51]. In the thesis I focused on the study of the properties of  $^{69}\text{Ni}$ , which has two isomeric states  $1/2^-$  ( $\nu(g_{9/2}^2)_0^+ \nu p_{1/2}$ ) and  $17/2^-$  ( $\nu(g_{9/2}^2)_8^+ \nu p_{1/2}$ ). I constrained the excitation energy of the  $17/2^-$  ( $E^*=2701$  keV) and determined its half-life ( $T_{1/2}=0.47$   $\mu\text{s}$ ). The  $1/2^-$  isomer was identified at an excitation energy  $E^*=321.5$  keV. This picture is supported by the similarity to the mirror valence nucleus on the neutron deficient side  $^{91}\text{Nb}$ , which has an identical sequence of levels at low excitation energies.

From the shell-model point of view the knowledge and understanding of the properties of  $^{71}\text{Cu}$  were particularly interesting, with its isomeric state at  $E^*=2755.5$  keV and having  $I^\pi=17/2^-$ . The proposed sequence of levels connected by intense E2 transitions shows a large similarity to the level sequence in  $^{70}\text{Ni}$ . Their systematics, which reflects the structure of a given nucleus, depends on the residual interaction of the valence nucleons, i.e. for  $^{70}\text{Ni}$  two neutrons on the  $g_{9/2}$  shell. The comparison of the decay schemes of  $^{71}\text{Cu}$  and  $^{70}\text{Ni}$  allows to state the lack of strong correlation between the neutron and the proton, which are located

on the  $\nu g_{9/2}$  and  $\pi p_{3/2}$  orbitals. On the other hand, strong coupling occurs between neutrons lying on the same  $\nu g_{9/2}$  shell [51].

### 5.1.2 DOCTORAL STUDIES

My doctoral thesis was centered around the study of  $N=84$  isotones ( $^{134}\text{Sn}$ ,  $^{135}\text{Sb}$ ,  $^{136}\text{Te}$ ,  $^{137}\text{I}$ ,  $^{138}\text{Xe}$ ) and the nuclei  $^{133}\text{Sn}$ ,  $^{134}\text{Sb}$  and  $^{139}\text{Cs}$ . These nuclei were produced in the spontaneous fission of  $^{248}\text{Cm}$  and the  $\gamma$  radiation emitted promptly following the fission was detected by means of the EUROGAM II array. Moreover, in order to correctly identify the transitions measured in the prompt fission data, a measurement of the excited states populated in the  $\beta^-$  decays at mass  $A=134$ ,  $135$ ,  $137$ , and  $139$  was done. These experiments were carried on at the OSIRIS separator in Studsvik using neutron induced fission of  $^{235}\text{U}$  and  $^{238}\text{U}$  to produce the isotopes of interest. The result of this work was the identification of a few tens of both low- and high-spin states in seven nuclei close to the doubly-magic nucleus  $^{132}\text{Sn}$ . The spin and parity of the states were assigned on the basis of angular correlations and linear polarization.

The advantage of combining data obtained in experiments in which yrast states are populated with data on excited states populated in  $\beta$  decay, allows to properly assign  $\gamma$  rays. In the analysis of prompt-fission  $\gamma$  rays the assignment to the isotope is usually based on known coincidences with known transitions in the prompt-fission partner. Depending on the number of evaporated neutrons in the fission process, different partners can correspond to one particular fission fragment. An example is the case of  $^{139}\text{Cs}$ . The cascade of transitions in this isotope was wrongly assigned as belonging to  $^{142}\text{Cs}$  in a previous work based only on data from fission [52]. It is important not to forget that in the fission process more than 200 different fragments are produced, each emitting prompt  $\gamma$  radiation. In the case of the (low-spin)  $\beta$ -decay data, the fission fragments were separated according to their mass number and then implanted in the centre of the detection set-up. The implantation point was surrounded by the detection set-up to register both  $\gamma$  rays and  $\beta$  particles. The new measurement of  $\beta$ -delayed  $\gamma$  rays and the correct analysis of prompt- $\gamma$  from fission of  $^{248}\text{Cm}$  allowed to correctly identify the cascade of  $\gamma$ -rays belonging to  $^{139}\text{Cs}$  [53].

The data presented in my doctoral thesis allowed to confirm the single-particle energy value for the  $\nu h_{9/2}$  and estimate for the first time the single-particle energy for the high-spin neutron state  $i_{13/2}$ . The energy of the  $\nu h_{9/2}$  was determined from the corresponding state in  $^{133}\text{Sn}$ , which has one neutron outside the close  $^{132}\text{Sn}$  core. A similar approach for  $\nu i_{13/2}$  was not possible, since theoretical predictions for this state in the  $^{132}\text{Sn}$  potential placed it above the neutron separation energy in that nucleus [54]. Our work concentrated on finding a bound state which is characterised by a simple structure, like, e.g., two valence particles on the  $\nu i_{13/2}$  and higher neutron separation energy. The result was the identification of an excited state in  $^{134}\text{Sb}$  which



has  $\pi g_{7/2} \nu i_{13/2}$  configuration. Unfortunately its excitation energy is not known with respect to the ground state, but only with respect to the  $I^\pi=7^-$  isomeric state. As a consequence, the single particle energy for the  $\nu i_{13/2}$  state, 2700(200) keV, suffers from large uncertainty.

In the PhD thesis I have also made a systematic analysis of the N=84 isotones in the vicinity of  $^{132}\text{Sn}$ . The goal of these studies was to probe the limits of applicability of the shell model in describing nuclei with several valence particles. This was done by comparing experimental excited-level sequences in those nuclei with theoretical calculations performed within the shell model. An interesting case is the  $I^\pi=12^+$  isomer predicted in  $^{136}\text{Te}$ , which is not observed experimentally. The presence of four valence nucleons in  $^{136}\text{Te}$  causes the core to "soften" to the level that the excited states are collective enough and cannot be described within the shell-model. A similar situation is found in  $^{137}\text{I}$ , in which an analogue isomer with  $I^\pi=29/2^+$  is predicted, but not observed. This means that at N=84 we already observe collective effects [55]. This conclusion is very significant for the prediction of properties of neutron-rich isotopes close to Z=50, close to the predicted path for the astrophysical r-process, which is obtained using predictions from the available models.

## 5.2 OTHER SCIENTIFIC INTERESTS AFTER THE END OF DOCTORAL STUDIES

### 5.2.1 PROPERTIES OF NEUTRON-DEFICIENT NUCLEI CLOSE TO $^{100}\text{Sn}$

On the neutron-deficient side of the chart of nuclei, a particularly interesting region is the one close to the doubly magic  $^{100}_{50}\text{Sn}_{50}$ . The isotopes that lie in its close vicinity are important not only because of their relevance for the astrophysical rp-process, but also because they offer the possibility to investigate the proton-neutron interaction. These nuclei are characterised by being  $\alpha$  and/or proton emitters because of their vicinity to the proton drip-line and the closed N=Z=50 shells. The study of their decay properties allows to gather information on their wave functions of the nuclear states involved in the decay. In this particular case, when the number of neutrons and protons is identical, the valence protons and neutrons are in the same orbitals and as a consequence the proton-neutron interaction is stronger. In the case of the isotopes lying just above  $^{100}\text{Sn}$ , which were the subject of my studies, the valence protons and neutrons occupy the same  $d_{5/2}$  or  $g_{7/2}$  orbitals. The overlap of the wave functions should increase the probability of formation and emission of  $\alpha$  particles in so-called "super-allowed" decays [56–58].

The study of  $^{100}\text{Sn}$  and nuclei in its immediate neighbourhood is particularly challenging and often non-possible because of the extremely small cross section for their production. For example, among the products of the fragmentation of a  $^{124}\text{Xe}$  beam (1 GeV/nucleon) [59] and a  $^{112}\text{Sn}$  beam (63 MeV/nucleon) [60, 61] only few ions of  $^{100}\text{Sn}$  were identified, 11 and 24, respectively.

In the publication [62] I tried to determine the optimal conditions for the production of nuclei around  $^{100}\text{Sn}$  in a fusion-evaporation reaction. In particular, I investigated the possibility to produce  $^{108}\text{Xe}$  in order to study the "super-allowed"  $\alpha$  decays in the chain  $^{108}\text{Xe} \rightarrow ^{104}\text{Te} \rightarrow ^{100}\text{Sn}$ . Using the code HIVAP I ran a series of calculations of the cross section for producing the isotopes  $^{108-112}\text{Xe}$ ,  $^{108-110}\text{I}$  and  $^{108-109}\text{Te}$  in the fusion-evaporation reaction of a  $^{58}\text{Ni}$  beam and a  $^{54}\text{Fe}$  target. The calculations were verified experimentally and on their basis I produced the excitation function curve for different reaction channels. The experiments were performed at the HRIBF facility, where in the reaction of a  $^{58}\text{Ni}$  beam and a  $^{54}\text{Fe}$  target, after evaporation of 0 – 3 neutrons,  $^{109-112}\text{Xe}$  were produced. The ions of interest were separated from the other reaction products by means of Recoil Mass Separator (RMS) and implanted into a double-sided silicon-strip detector installed at the focal plane, where their decay was recorded. By comparing the results of the cross section measurements with the results of the calculations, I determined the optimal beam energy for production of  $^{108}\text{Xe}$  in the reaction  $^{58}\text{Ni}(^{54}\text{Fe},4n)^{108}\text{Xe}$ : the beam energy should be 240 MeV, corresponding to excitation energy of 58 MeV in the compound nucleus  $^{112}\text{Xe}$  [62]. At this beam energy, the production cross-section for  $^{108}\text{Xe}$  is about 1 nb, which, under realistic assumptions for beam energy and target thickness, gives a production rate of about 20  $^{108}\text{Xe}$  ions every 100 hours. While implementing the research program to study nuclei in the vicinity of  $^{100}\text{Sn}$ , I prepared and took part in several experiments, including that which led to the identification of the new isotope  $^{109}\text{Xe}$  and its  $\alpha$  decay chain  $^{109}\text{Xe} \rightarrow ^{105}\text{Te} \rightarrow ^{101}\text{Sn}$  [57] and the one which found a weak  $\alpha$ -decay branch ( $1.4 \times 10^{-4}$ ) in the proton emitter  $^{109}\text{I}$  [63].

### 5.2.2 RARE DECAY MODES OF EXOTIC NUCLEI

Shortly after the doctoral studies I got engaged in the pioneering research on two-proton ( $2p$ ) radioactivity carried on at the Nuclear Physics Division at FUW. The measurement of the two protons emitted in  $2p$  decay was possible thanks to the development of a new detector (at FUW), a time-projection chamber with optical readout (OTPC). The OTPC detector allows to measure and reconstruct in 3D the trajectories of charged particles in the active volume of the detector. The advantage of the OTPC with respect to standard silicon detectors is the very low energy threshold for registering the signals and the very high sensitivity of the system that allows to identify the decay even when only one event is detected. The OTPC detector is ideally suited to study rare decay modes of exotic proton-rich nuclei. The most spectacular results obtained with the use of the OTPC detector are the first direct observation of  $2p$  radioactivity of  $^{45}\text{Fe}$  [64], after its discovery in 2002, and the identification of the emission of three protons following  $\beta$  decay of  $^{43}\text{Cr}$  [65]. My contribution in this research consisted in the preparation of the experiment and participation in the measurement. More recently, the OTPC detector was used to study the next candidates for  $2p$  decay, namely the  $^{59}\text{Ge}$  and  $^{60}\text{Ge}$  iso-

topes. I took part in the experiment at the NSCL laboratory at the A1900 spectrometer, when the  $^{59}\text{Ge}$  [66] isotope was discovered and the first decay properties of  $^{60}\text{Ge}$  measured (half life and delayed proton emission probability) [67].

### 5.2.3 STRUCTURE OF NUCLEI CLOSE TO THE SEMI-MAGIC $^{68}\text{Ni}$ .

For neutron number between  $N=28$  and  $N=40$  changes in the excitation energy of the nuclei are given by neutrons filling the  $\nu p_{3/2}$ ,  $\nu f_{5/2}$  and  $\nu p_{1/2}$  orbitals. After crossing the  $N=40$  line the  $\nu g_{9/2}$  orbital becomes active. The semi-magicity of  $N=40$  is reflected in the high excitation energy of the first  $2^+$  state (2034 keV) and its low  $B(E2)=3.2(7)$  W.u in  $^{68}\text{Ni}_{40}$ . The reduced transition probability  $B(E2)$  is comparable with doubly magic nuclei like, e.g.,  $^{16}\text{O}$  (3.3(3) W.u.),  $^{40}\text{Ca}$  (2.3(4) W.u.) and  $^{48}\text{Ca}$  (1.6(5) W.u.) [37].

The filling of the  $\nu g_{9/2}$  orbit causes the change in the splitting of the proton orbits  $\pi f_{5/2}-\pi f_{7/2}$  (Figure 1c), which was experimentally confirmed in our work on the copper isotopes. In the following work I focussed on the study of excited states in  $^{71}\text{Zn}_{41}$ , which has two neutrons and one proton outside the  $^{68}\text{Ni}$  core, and proposed an experiment to measure it using  $^{70}\text{Zn}(n,\gamma)$  reaction to populate the excited states. The experiment was performed at the ILL laboratory in Grenoble and provided the first  $(n,\gamma)$  measurement using a  $^{70}\text{Zn}$  target. Its results yielded the identification of more than 200 new transitions corresponding to the de-excitation of excited states in  $^{71}\text{Zn}$ . On the basis of angular correlations the spin and parity of several states could be determined. The data analysis was conducted under my supervision within the framework of a master thesis. At present we are completing the theoretical interpretation of the results, which will be published soon together with the experimental results.

### 5.2.4 PROPERTIES OF NUCLEI STUDIED WITH THE FAST TIMING TECHNIQUE

$\beta$  decay populates excited states in the daughter nucleus that de-excite to the ground state by emission of (a cascade of)  $\gamma$  rays. In order to understand the structure of the nucleus investigated, it is necessary to know not only the energy of the emitted  $\gamma$  rays, but also other properties of the nucleus, like for example the lifetime of the excited states. One of the challenges in a lifetime measurement is its broad range, which can span orders of magnitude, down to the sub-nanoseconds range. Another challenge is given by the large multiplicity with the simultaneous emission of a several  $\gamma$  rays, which make the selection of the interesting events among all those registered not easy. For these reasons, the measurement of sub-nanosecond lifetimes of excited states populated in  $\beta$  decay required the development of a special measurement technique  $\beta - \gamma - \gamma(t)$  [24-26]. This technique was applied also in the work described in section 4.33. Triple coincidences of the  $\beta$  particle with  $\gamma$  rays detected in a fast scintillator

detector and  $\gamma$  rays registered in a detector with worse time resolution but very good energy resolution, are measured. The scintillator detectors provide information on the delay of the  $\gamma$ -ray emission with respect to the  $\beta$  particle, the other  $\gamma$ -ray detector ensures the identification and selection of the correct  $\gamma$ -ray cascade. The  $\beta - \gamma - \gamma(t)$  technique allows to measure the lifetime of states populated in  $\beta$  decay in the range nano- to picosecond and is a universal method, which can be used to study unstable nuclei independently on their location on the map of nuclei. The measurement of the lifetime of levels, of the energy of the emitted  $\gamma$ s and of the branching ratio allow to determine the matrix elements  $B(XL)$  for the  $\gamma$  transition de-exciting the studied state. The analysis of these observables allows to constrain the character of the excited state (collective versus single particle).

The measurement of the lifetimes of nuclear excited states provide a series of important pieces of information on the structure of atomic nuclei. I took part in measurements which, among others, showed that the addition of a few valence nucleons to the magic core causes a rapid change in the properties of the nucleus: from spherical nuclei, which are well described by the shell model, to nuclei in which the migration of single-particle states can be observed ( $^{32}\text{Mg}$  [68],  $^{30}\text{Mg}$  [69],  $^{66}\text{Fe}$  [70],  $^{67}\text{Cu}$ ,  $^{100}\text{Zr}$ ), to the region of strong octupole correlations ( $^{96}\text{Zr}$ ,  $^{146}\text{Ba}$  [71],  $^{224}\text{Ra}$  [72]). We obtained interesting results also for  $^{94}_{44}\text{Ru}_{50}$  and  $^{96}_{46}\text{Pd}_{50}$  [73]. The measurement of the lifetimes of low-lying excited states in these nuclei showed for the first time the inadequacy of the seniority quantum number to describe the configuration  $\pi g_{9/2}^n$  in the  $N=50$  isotones. Particle-hole neutron excitations through the  $N=50$  shell are responsible for this effect.

A complementary method with respect to the lifetime measurement to gather information on the matrix elements of electromagnetic transitions in nuclei is given by coulomb excitations. This well known technique is living its *renaissance* thanks to the advent of radioactive beams. I participated in such research conducted in Warsaw at the Heavy Ion Laboratory. The experiment to investigate coulomb excitation of  $^{118}\text{Sn}$  was run in June 2017.

## REFERENCES

- [1] M. Goepfert, Phys. Rev. **78**, 16 (1950).
- [2] T. Mayer-Kuckuk *Fizyka jądrowa*, PWN 1983 r.
- [3] H. Grawe, K. Langanke, G. Martinez-Pinedo  
Rep. Prog. Phys. **70**, 1525 (2007).
- [4] T. Otsuka Phys. Scr. **T152**, 014007 (2013).
- [5] T. Otsuka *et al.*, Phys. Rev. Lett. **95**, 232502 (2005).
- [6] T. Otsuka *et al.*, Phys. Rev. Lett. **87**, 082502 (2001).
- [7] H. Simon *et al.*, Phys. Rev. Lett. **83**, 496 (1999).
- [8] T. Otsuka *et al.*, Phys. Rev. Lett. **104**, 012501 (2010).
- [9] R. Kanungo *et al.*, Phys. Rev. Lett. **102**, 152501 (1999).
- [10] D. Steppenbeck *et al.*, Nature **502**, 207 (2013).
- [11] J. Dobaczewski *et al.*, Phys. Rev. Lett. **72**, 981 (1994).
- [12] J. Dobaczewski *et al.*, Phys. Rev. C **53**, 2809 (1996).
- [13] J. Dobaczewski *et al.*, Progress Part. Nucl. Phys. **59**, 432 (2007).
- [14] N.A. Smirnova *et al.*, Phys. Lett. B **686**, 109 (2010).
- [15] K.T. Flanagan *et al.*, Phys. Rev. Lett. **103**, 142501 (2009).
- [16] S.V. Ilyushkin ... A. Korgul *et al.*, Phys. Rev. C **80**, 054304 (2009).
- [17] S.V. Ilyushkin ... A. Korgul *et al.*, Phys. Rev. C **83**, 014322 (2011).
- [18] J. M. Daugas *et al.*, Phys. Rev. C **75** 034304 (2010).
- [19] K. Sieja and F. Nowacki Phys. Rev. C **81**, 061303(R) (2010).
- [20] M. Madurga, ... A. Korgul *et al.*, Phys. Rev. Lett. **109**, 112501 (2012).
- [21] J.A. Winger, ... A. Korgul *et al.*, Phys. Rev. Lett **102**, 142502 (2009).
- [22] C.J. Gross *et al.*, Eur. Phys. J. A **25**, s01, 115 (2005).

- [23] J.A. Winger, ... A. Korgul *et al.*, Phys. Rev. C **81**, 044303 (2010).
- [24] H. Mach *et al.*, Nucl. Phys. A **523**, 197 (1991).
- [25] H. Mach, R. Gill and M. Moszynski, Nucl. Instrum Methods A **280**, 49 (1989).
- [26] M. Moszynski and H. Mach, Nucl. Instrum Methods A **277**, 407 (1989).
- [27] W. Urban *et al.*, Z. Phys. A **358**, 145 (1997).
- [28] K. Sieja *et al.*, Phys. Rev. C **79**, 064310 (2009).
- [29] K. Sieja *et al.*, Phys. Rev. C **88**, 034327 (2013).
- [30] [http://www-phynu.cea.fr/science\\_en\\_ligne/carte\\_potentiels\\_microscopiques/carte\\_potentiel\\_nucleaire.htm](http://www-phynu.cea.fr/science_en_ligne/carte_potentiels_microscopiques/carte_potentiel_nucleaire.htm)
- [31] W. Rae, NUSHELLX shell-model code,  
<http://www.garsington.eclipse.co.uk/>.
- [32] M. Hjorth-Jensen, T. T. S. Kuo, and E. Osnes, Phys. Rep. **261**, 125 (1995).
- [33] R. Machleidt, arXiv:0704.0807 [nucl-th].
- [34] M. F. Alshudifat, ... A. Korgul *et al.*, Phys. Rev. C **93**, 044325 (2016).
- [35] M.-G. Porquet *et al.*, Eur. Phys. J. A **40**, 131 (2009).
- [36] W. Urban *et al.*, Phys. Rev. C **94**, 044328 (2016).
- [37] <http://www.nndc.bnl.gov>
- [38] K. Miernik, ... A. Korgul *et al.*, Phys. Rev. Lett **111**, 132502 (2013).
- [39] M. Czerwiński *et al.*, Phys. Rev. C **88**, 044314 (2013).
- [40] M. Sanchez-Vega *et al.* Phys. Rev. Lett. **80**, 25 (1998).
- [41] J. Shergur *et al.*, Phys. Rev. C **65**, 034313 (2002).
- [42] M. Sanchez-Vega *et al.*, Phys. Rev. C **60**, 024303 (1999).
- [43] J. Blomqvist Proceedings of the 4<sup>th</sup> International Conference on Nuclei far from Stability, Helsingør, Denmark, (CERN report 81-09, Geneva 1981, s.536)(1981).
- [44] P. Hoff *et al.* Phys. Rev. Lett. **77**, 1020 (1996).

- [45] W. Urban, ... A. Nowak *et al.* Eur. Phys. J A **5**, 239 (1999)
- [46] J. Shergur *et al.*, Phys. Rev. C **71**, 064321 (2005).
- [47] K.A. Mezilev *et al.*, Phys.Scripta **T56**, 272 (1995).
- [48] J. Van Schelt *et al.*, Phys. Rev. C **85**, 045805 (2012).
- [49] J. Van Schelt *et al.*, Phys. Rev. Lett. **111**, 061102 (2013).
- [50] W. Reviol *et al.*, Phys. Rev. C **94**, 034309 (2016).
- [51] R. Grzywacz,..., A. Nowak *et al.* Phys. Rev. Lett. **81**, 766 (1998).
- [52] J.K. Hwang *et al.*, Phys. Rev. C**57**, 2250 (1998).
- [53] A. Nowak *et al.*, Eur. Phys. J. A**6**, 1 (1999).
- [54] J.-Y. Zhank *et al.*, Phys. Rev. C**58**, R2663 (1998).
- [55] A. Korgul *et al.*, Eur. Phys. J. A**7**, 167 (2000).
- [56] R.D. Macfarlane and A. Siivola, Phys. Rev. Lett. **14**, 114 (1965).
- [57] S.N. Liddick, ... A. Korgul *et al.*, Phys. Lett. **B97**, 082501 (2006).
- [58] C. Xu and Z. Ren Phys. Rev. C **74**, 037302 (2006).
- [59] R. Schneider *et al.*, Z. Phys. A **384**, 241 (1994).
- [60] M. Lewitowicz *et al.*, Phys. Lett. **B332**, 20 (1994).
- [61] K. Rykaczewski *et al.*, Phys. Rev. C **52**, R2310 (1995).
- [62] A. Korgul *et al.*, Phys. Rev. C **77**, 034301 (2008).
- [63] C. Mazzocchi, ... A. Korgul *et al.* Phys. Rev. Lett. **98**, 212501 (2007).
- [64] M. Pfützner *et al.*, Eur. Phys. J A **14**, 279 (2002).
- [65] M. Pomorski,... A. Korgul *et al.*, Phys. Rev. C **83**, 014306 (2011).
- [66] AA. Ciemny,... A. Korgul *et al.*, Phys. Rev. C **92**, 014622 (2015).
- [67] AA. Ciemny,... A. Korgul *et al.*, Eur. Phys. J A **52**, 89 (2016).
- [68] H. Mach, ..., A. Korgul *et al.*, Eur. Phys.J. A **25**, s01, 105 (2005).

- [69] B. Olaizola, ..., A. Korgul *et al.*, Phys. Rev. C. **94**, 054318 (2016)
- [70] B. Olaizola *et al.*, Phys.Rev. C **88**, 044306 (2013).
- [71] H. Mach *et al.*, Phys.Rev. C **41**, R2469 (1990).
- [72] L.M. Fraile *et al.*, Nucl.Phys. A **657**, 355 (1999).
- [73] H. Mach, A. Korgul *et al.*, Phys. Rev. C. **95**, 014313 (2017).



Warsaw August 28, 2017 r.